RSC Chemical Biology

ROYAL SOCIETY OF CHEMISTRY

COMMUNICATION

View Article Online
View Journal | View Issue

Cite this: *RSC Chem. Biol.*, 2025, **6**, 1832

Received 19th July 2025,
Accepted 10th October 2025

DOI: 10.1039/d5cb00187k

rsc.li/rsc-chembio

Alkyne-tagged ribitol-5-phosphate derivatives for metabolic labelling of alpha-dystroglycan

Lloyd D. Murphy,[a] Saeed Akkad,[a] Angelo Lopez,[a] Morgan E. Batiste-Simms,[a] Greg L. McNeil,[a] Eva W. Wan,[b] Kathryn E. Huxley,[a] Luke Julyan,[b] Mia Shandell[a] and Lianne I. Willems *[a]

The glycoprotein α-dystroglycan is essential in establishing cell-matrix interactions and is implicated in the pathology of muscular dystrophies. Novel tools are needed to study its rare and intriguing *O*-mannosyl glycans. This report describes the synthesis and evaluation of alkyne-tagged ribitol-5-phosphate derivatives for the metabolic labelling of α-dystroglycan in mammalian cells.

O-Mannosylation is a type of *O*-linked glycosylation that is initiated by the addition of an α-linked D-mannose residue onto serine or threonine hydroxyl groups and is conserved from bacteria to humans.[1,2] In mammals, the initial mannose residue can be extended and/or branched to give three different oligosaccharide core structures termed core M1, M2 and M3.[3] Core M3 glycans provide an attachment site for matriglycan, a glycosaminoglycan-like structure that consists of a linear chain of repeating Xylα1,3-GlcAβ1,3-disaccharides and acts as a receptor for proteins containing laminin globular domains (Fig. 1A and B).[4,5] The matriglycan-carrying core M3 glycans are exclusively found on the heavily glycosylated cell surface protein α-dystroglycan (α-DG), which forms part of the dystrophin-glycoprotein complex that anchors the intracellular cytoskeleton to the extracellular matrix (ECM) (Fig. 1A).[6] The laminin-binding ability of matriglycan is critical in mediating interactions between this complex and the ECM.[4,7,8] Due to the importance of these glycans in neuromuscular tissue, defects in their biosynthesis lead to a group of debilitating congenital muscular dystrophies termed alpha-dystroglycanopathies.[6]

Biosynthesis of core M3 glycans begins in the endoplasmic reticulum with formation of the phosphorylated trisaccharide GalNAc-β1,3-GlcNAc-β1,4-Man-6-phosphate.[9] This structure can be extended further in the Golgi apparatus, culminating with the addition of the matriglycan chain. Notably, the linker between the core glycan and matriglycan chain contains a unique structural feature consisting of two tandem phosphodiester-linked D-ribitol-5-phosphate (Rbo5P) residues (Fig. 1B),[10–12] which are not known to be present in any other mammalian glycoconjugates. The length of the matriglycan chain varies significantly across tissues and cell types and is known to play an important role in tuning ECM binding.[7,13] Despite the recognised biological importance of these glycans, however, details of different glycoforms and how their biosynthesis and turnover are regulated remain unclear.

One of the major challenges in studying α-DG is the limited availability of tools to probe and manipulate glycosylated α-DG in a native context. Detection commonly involves the use of laminin overlay assays or IIH6 antibodies, which recognise the matriglycan epitope.[14] These approaches suffer from variable affinity and fail to detect glycoforms with a shorter matriglycan chain.[15] Additionally, the high molecular weight and anionic nature of matriglycan make isolation and mass spectrometry analysis of the glycopeptides very challenging.[16] Access to novel tools that enable the covalent tagging of α-DG in a cellular context, improving detection and enrichment efficiency, would greatly benefit further research into its glycans.

Capitalising on the exclusive presence of Rbo5P in core M3 glycans, we set out to develop a chemical reporter strategy using Rbo5P analogues for the metabolic labelling of α-DG (Fig. 1C).[17] For this purpose, we designed ribitol and Rbo5P derivatives that are equipped with a bioorthogonal alkyne tag (Fig. 2). Cellular uptake of these probes, metabolic conversion into glycosylation donors and assimilation into the native core M3 biosynthesis pathway will lead to alkyne-tagged glycans, which can be selectively labelled *via* copper(I)-catalysed azide–alkyne cycloaddition ('click' reaction) (Fig. 1C). Here, we describe the synthesis of alkyne-tagged probes **1–4** (Fig. 2) and demonstrate successful fluorescent labelling of overexpressed α-DG with the Rbo5P-derived probes **1** and **2**.

Results and discussion

Rbo5P is incorporated into core M3 glycans by the sequential action of two ribitol-phosphate transferases, fukutin (FKTN)

[a] *York Structural Biology Laboratory and York Biomedical Research Institute, Department of Chemistry, University of York, York YO10 5DD, UK. E-mail: lianne.willems@york.ac.uk*
[b] *Department of Chemistry, University of York, York YO10 5DD, UK*

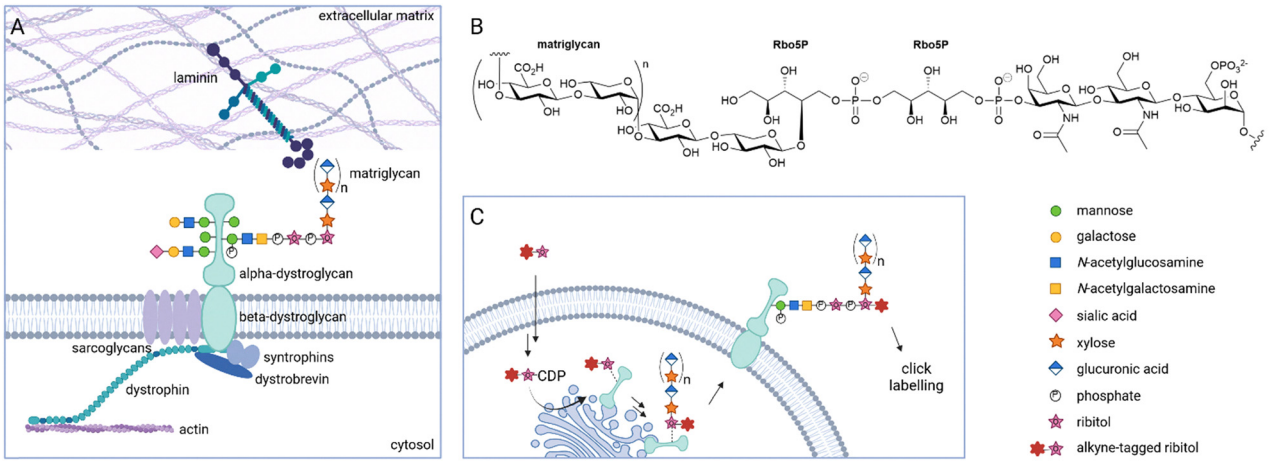

Fig. 1 A chemical reporter strategy to interrogate glycosylation of the mammalian protein α-dystroglycan (α-DG). (A) *O*-Mannosylation of α-DG, in particular formation of core M3 glycans carrying the matriglycan motif, is essential for the laminin-binding function of the dystrophin-glycoprotein complex. (B) Structure of a core M3 glycan fully extended with matriglycan and containing two tandem ribitol-5-phosphate (Rbo5P) residues. (C) Metabolic glycan engineering with tagged Rbo5P derivatives. Upon cellular uptake, the probes are metabolically converted into cytidine diphosphate (CDP)-activated glycosylation donors and incorporated into core M3 glycans on α-DG.

and fukutin-related protein (FKRP).[10,11] These enzymes use cytidine diphosphate (CDP)-ribitol as a donor, which is generated from Rbo5P by isoprenoid synthase domain-containing protein (ISPD).[10–12,18] Multiple pathways towards Rbo5P appear to coexist in mammalian cells, including *via* the phosphorylation of ribitol or through reduction of ribose-5-phosphate or ribulose-5-phosphate.[10,19,20] While this suggests ribitol could be used as a probe scaffold, we focused our strategy on Rbo5P-based probes because of the uncertainty in the metabolic fate of the pentitol sugar. It has also been shown that using more advanced metabolic intermediates can result in enhanced metabolic labelling efficiency.[21–23] We opted to add the alkyne tag onto the synthetically easily accessible C1 position of the Rbo5P backbone (with carbon numbering following the standard nomenclature for ribose-5-phosphate). In probe **1**, the molecule's native hydroxylation pattern is retained, while in **2** the C1 hydroxyl group is substituted to generate a slightly shorter probe (Fig. 2). We also included the ribitol analogues **3** and **4** for comparison of their labelling efficiency with that of their phosphorylated counterparts **1** and **2**. To enhance cell permeability of the probes, biolabile acetyl and *S*-acyl-2-thioethyl (SATE) protecting groups are installed.[24] SATE protection is a common strategy in the design of nucleoside monophosphate and phosphonate prodrugs[25,26] and has also been successfully applied to metabolic glycan engineering.[21–23,27,28] Upon cellular uptake, esterase-mediated hydrolysis of the thioesters generates mercaptoethyl groups that spontaneously decompose to release the free phosphate.

The synthetic strategy towards probes **1–4** starts from D-ribose (Scheme 1). We reasoned that conversion to the benzylated aldehyde intermediate **5** would allow introduction of the alkyne at the C1 position *via* a Corey–Fuchs or a Grignard reaction, leading to the required 6- and 7-carbon probe backbones (**7** and **6**, respectively). To facilitate selective installation of the bis-SATE-protected phosphotriester onto the primary hydroxyl group (corresponding to the C5–OH of ribitol),

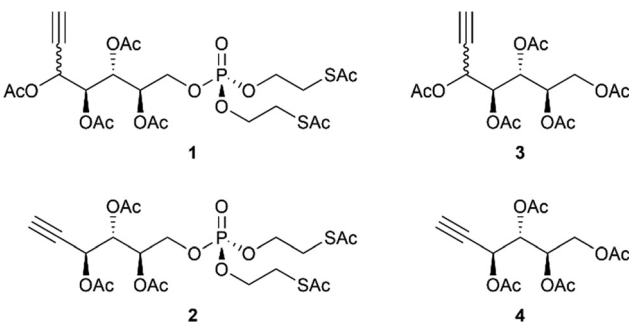

Fig. 2 Structures of alkyne-tagged ribitol and Rbo5P derivatives synthesised in this study for the metabolic labelling of Rbo5P-containing glycans.

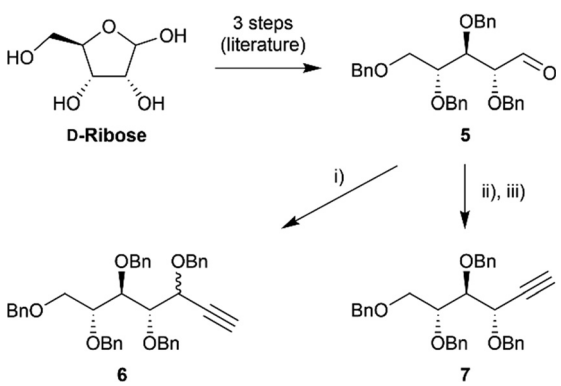

Scheme 1 Synthesis of alkyne-tagged probe scaffolds. (i) Ethylmagnesium bromide, TMS-acetylene, THF, −78 °C to rt; then NaH, BnBr, THF, 0 °C to rt, 58% over two steps (dr 3.5 : 1). (ii) CBr_4, PPh_3, Et_3N, CH_2Cl_2, −10 °C to rt, 84%. (iii) LDA, THF, 72%.

regioselective debenzylation can be performed, avoiding the need for a lengthier orthogonal protecting group strategy.

Thus, aldehyde **5** (Scheme 1) was synthesised from D-ribose following literature procedures.[29,30] The alkyne tag was then introduced using a Grignard reagent generated *in situ* from TMS-acetylene and ethylmagnesium bromide, followed by benzylation of the resulting hydroxyl group to yield compound **6** as a mixture of diastereomers which were not separated during purification (see SI for experimental procedures). Since it is unknown if the enzymes involved in cellular processing of the unnatural pentitol phosphate have a preference for either of the diastereomers, the synthesis was continued with the product mixture. Alternatively, the alkyne was introduced using a two-step Corey–Fuchs protocol, involving formation of a dibromoolefin intermediate which upon treatment with lithium diisopropylamide afforded compound **7**.

To allow for regioselective incorporation of the phosphate ester, the primary benzyl ether in compounds **6** and **7** was deprotected by selective conversion into an acetyl ester using $ZnCl_2$ in the presence of acetic anhydride and acetic acid, followed by ester hydrolysis to give compounds **8a** (from **6**) and **8b** (from **7**) (Scheme 2).[31] The resulting hydroxyl group was converted into a bis-SATE protected phosphotriester with phosphorus(V) chemistry using our recently published procedure.[32] Briefly, triflic anhydride/pyridine-mediated reaction with tri(2-bromoethyl) phosphate afforded **9a**/**9b**, after which substitution of the bromides by thioacetate gave **10a**/**10b**. To complete the synthesis, debenzylation and acetylation of the hydroxyl groups yielded the desired probes **1** and **2**. In addition, probes **3** and **4** were obtained by debenzylation and acetylation of compounds **6** and **7**.

The ability of the synthesised molecules **1–4** to act as metabolic labelling probes was tested in human embryonic kidney (HEK) cells overexpressing α-DG. Stably transfected, doxycycline-inducible HEK293F cells were generated using the piggyBac transposon-based expression system.[33] For this purpose, we used a previously reported, N-terminally FLAG-tagged α-DG construct.[34] Endogenous α-DG is formed by proteolytic cleavage of the precursor protein dystroglycan into two subunits, of which α-DG localises extracellularly and interacts non-covalently with the transmembrane subunit β-DG. It is well established that α-DG can be expressed in the absence of the β-subunit and is then, in its fully glycosylated form, secreted into the culture media.[34–36] Successful production of the target protein and its secretion into the conditioned media over several weeks after the start of induction was validated by SDS-PAGE and western blot analysis (Fig. S1A and B). FLAG-tagged α-DG has a predicted molecular weight of 69 kDa without glycans. Its appearance as a broad band around ~130 kDa is consistent with its extensive level of glycosylation. Additionally, the fact that it can be detected by the matriglycan-specific IIH6 antibody (Fig. S1A) confirms that HEK293F cells possess the required machinery for the biosynthesis of matriglycan-carrying core M3 glycans. Anti-FLAG immunopurification resulted in detection of the same protein band as well as a more slowly migrating signal (Fig. S2A). LC-MS/MS analysis of the excised gel bands confirmed the identity of the immunopurified protein as α-DG (Table S1).

Using the inducible FLAG-α-DG overexpression cell line, metabolic labelling with probes **1–4** was evaluated. Two days after induction of α-DG expression, cells were treated with one of the four probes for 34 hours. To visualise the incorporation of alkyne-tagged Rbo5P residues, FLAG-tagged α-DG was immunopurified from the culture media and labelled *via* click reaction with Cy5-picolyl azide for detection *via* in-gel fluorescence (Fig. 3 and Fig. S3). A distinct broad fluorescent band was observed at the expected molecular weight of α-DG after treatment of induced cells with probes **1** or **2**. This suggests successful incorporation of the alkyne-tagged Rbo5P derivatives into the target glycoprotein. In contrast, click labelling of non-probe treated controls did not result in any significant fluorescent signal, confirming the absence of non-specific labelling by the azido fluorophore. Additionally, non-induced control samples showed minimal fluorescence upon probe treatment and click reaction, demonstrating a low level of background labelling in the absence of α-DG overexpression.

By comparison, labelling with probes **3** and **4** failed to result in any specific Cy5 fluorescence (Fig. 3), indicating that these probes are not incorporated into α-DG glycans at detectable levels. Since metabolic conversion of these probes would yield the same alkyne-tagged CDP-ribitol derivatives as probes **1** and **2**, the lack of labelling suggests that the non-phosphorylated probes are not efficiently converted into the respective CDP-activated donors. These results highlight the critical role of the SATE-protected phosphate in enabling efficient cellular processing of Rbo5P precursors.

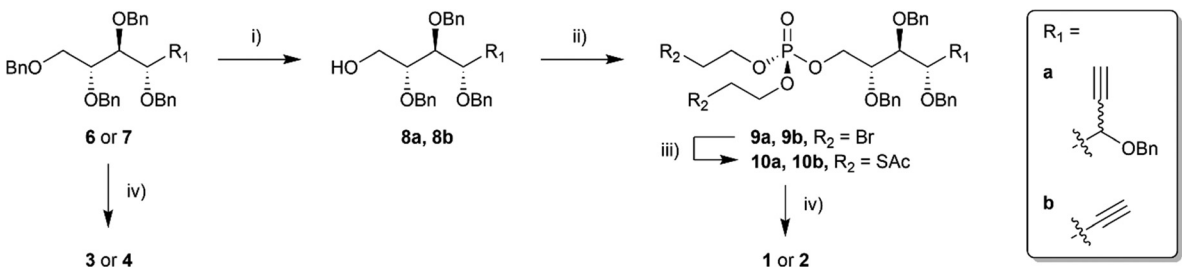

Scheme 2 Synthesis of target probes **1–4**. (i) $ZnCl_2$, Ac_2O, AcOH, 0 °C to rt; then K_2CO_3, MeOH, rt, **8a**: 71% (dr 3 : 1), **8b**: 68% over two steps. (ii) $OP(OCH_2CH_2Br)_3$, Tf_2O, pyridine, CH_2Cl_2, rt, **9a**: 65% (dr 3 : 1), **9b**: 57%. (iii) KSAc, pyridine, rt, **10a**: quantitative (dr 3 : 1), **10b**: quantitative. (iv) BCl_3, CH_2Cl_2, −78 °C; then Ac_2O, pyridine, rt, **1**: 31% (dr 7 : 1), **2**: 34%, **3**: 85% (dr 10 : 1), **4**: 57% over two steps.

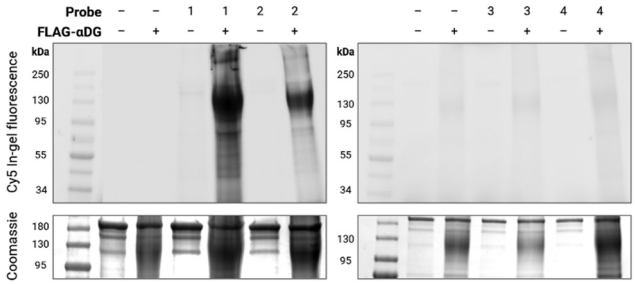

Fig. 3 Metabolic labelling of α-DG in mammalian cells. PiggyBac transposon-generated HEK293F cells expressing FLAG-tagged α-DG were induced with doxycycline and treated with 200 μM of probes **1–4** for 34 hours. Media were collected and immunoprecipitated with anti-FLAG resin. Click reaction was performed on-resin with Cy5-picolyl azide, after which proteins were eluted, resolved on SDS-PAGE and detected by in-gel fluorescence (top) and Coomassie staining (bottom). Non-induced cells ('– FLAG-αDG') and non-probe treated cells ('– probe') were included as controls.

The two Rbo5P units in the fully extended core M3 glycan are connected by a phosphodiester linkage between the 1- and 5-positions of the first and second ribitol residue, respectively (Fig. 1B). Therefore, we expected that incorporation of probe **2** as the first of the two Rbo5P residues in the glycan chain would preclude further glycan extension, since it lacks the C1 hydroxyl group of ribitol. Yet there is no obvious difference in the molecular weight of the fluorescent signal observed with probes **1** and **2**, which corresponds to fully glycosylated matriglycan-carrying α-DG. We infer that the alkyne-tagged Rbo5P derivatives may be incorporated more efficiently by FKRP than by FKTN, resulting in the probes being added as the second residue of the tandem Rbo5P linker, which enables further glycan extension to take place. It is also possible that cells can compensate for probe-triggered truncation of a core M3 glycan by forming a second, full-length (untagged) glycan at a different glycosylation site. Indeed, there are two core M3 glycosylation motifs within the mucin domain of α-DG at which the matriglycan-extended glycan has been identified (T317/T319 and T379/T381 in human α-DG).[15,16]

To validate the specificity of the observed labelling, we treated non-induced cells with probe **1**, allowing cellular uptake and metabolism of the probe to take place in the absence of α-DG overexpression, and collected the media. Then we mixed these with media from induced cells that had not been exposed to the probe and performed anti-FLAG immunopurification and click labelling on the combined media. Pleasingly, only low intensity fluorescent background labelling was observed (Fig. S4A). Similarly, addition of probe **1** to the isolated media of non-probe treated, induced cells directly before immunopurification did not result in labelling of α-DG (Fig. S4A). These results indicate that α-DG labelling by the alkyne-tagged Rbo5P derivatives requires the presence of the cell's glycan biosynthesis machinery and is not due to non-specific interactions between α-DG and the probe, supporting the specificity of the metabolic labelling approach.

Finally, the labelling selectivity was investigated by performing click reactions directly on the cell surface and in extracts of induced cells treated with probe **1** (Fig. S4B). While α-DG was not immunopurified and consequently could not be detected in this experiment, the results confirmed the absence of background labelling at the cell surface. In cell extracts, a few weakly labelled proteins were visible, the identity of which remains unknown and will be subject of future investigations.

Conclusions

We have developed a novel synthetic strategy to access alkyne-tagged ribitol and Rbo5P derivatives. In addition, we have demonstrated that the SATE-protected phosphorylated probes **1** and **2** facilitate labelling of overexpressed α-DG in mammalian cells, representing the first reported example of a ribitol-based chemical reporter strategy. Further optimisation is ongoing to improve labelling efficiency such that endogenous protein levels can be detected. Since α-DG is the only mammalian glycoprotein currently known to carry Rbo5P-containing glycans, our approach provides a valuable tool to study glycosylation in a protein-specific context. This metabolic labelling strategy has the potential to open new avenues for investigating the unique *O*-mannosyl glycans on α-DG and evaluating the effects of novel therapeutic strategies that are being explored to treat alpha-dystroglycanopathies, including ribose and ribitol supplementation.[37,38]

Author contributions

L. D. M. investigation; methodology; validation; visualisation; data curation; writing – original draft; writing – review & editing. S. A. investigation; methodology; visualisation; resources; data curation. A. L. investigation; methodology; resources; writing – review & editing. M. E. B.-S., G. L. M. and E. W. resources. K. E. H., L. J. and M. S. methodology. L. I. W. conceptualisation; funding acquisition; writing – original draft; writing – review & editing; visualisation; supervision; project administration.

Conflicts of interest

There are no conflicts to declare.

Data availability

Data associated with this publication, including unprocessed NMR data for all novel research compounds, raw images of gels and western blots, and the full list of proteins identified by LC-MS/MS analysis of digested gel bands, are available for download from the research data repository of the University of York at **https://doi.org/10.15124/0349da60-fafc-44e2-89c7-3d0c97962959**.

Supplementary information: supporting figures and tables, experimental procedures and NMR spectra of all new compounds. See DOI: **https://doi.org/10.1039/d5cb00187k**.

Acknowledgements

This work was funded by the European Research Council (ERC) under the European Union's Horizon 2020 research and innovation programme [Grant agreement no. 851448]. The authors thank professor Paul Martin (The Ohio State University College of Medicine) for his kind gift of the pFLAG-CMV2 alpha-dystroglycan expression plasmid and professor Gavin Wright (University of York) for the plasmids required to establish the piggyBac transposon-based expression system. LC-MS/MS analysis was performed at the York Centre of Excellence in Mass Spectrometry, which was created thanks to a major capital investment through Science City York, supported by Yorkshire Forward with funds from the Northern Way Initiative, and subsequent support from EPSRC (EP/K039660/1; EP/M028127/1). Fig. 1 was created in BioRender. **https://BioRender.com/8323o2a**.

References

1 M. Lommel and S. Strahl, *Glycobiology*, 2009, **19**, 816.
2 M. Koff, P. Monagas-Valentin, B. Novikov, I. Chandel and V. Panin, *Glycobiology*, 2023, **33**, 911.
3 J. L. Praissman and L. Wells, *Biochemistry*, 2014, **53**, 3066.
4 K. Inamori, T. Yoshida-Moriguchi, Y. Hara, M. E. Anderson, L. Yu and K. P. Campbell, *Science*, 2012, **335**, 93.
5 T. Yoshida-Moriguchi and M. P. Campbell, *Glycobiology*, 2015, **25**, 702.
6 M. Kanagawa, *Int. J. Mol. Sci.*, 2021, **22**, 13162.
7 M. M. Goddeeris, B. Wu, D. Venzke, T. Yoshida-Moriguchi, F. Saito, K. Matsumura, S. A. Moore and K. P. Campbell, *Nature*, 2013, **503**, 136.
8 D. C. Briggs, T. Yoshida-Moriguchi, T. Zheng, D. Venzke, M. E. Anderson, A. Strazzulli, M. Moracci, L. Yu, E. Hohenester and K. P. Campbell, *Nat. Chem. Biol.*, 2016, **12**, 810.
9 T. Yoshida-Moriguchi, T. Willer, M. E. Anderson, D. Venzke, T. Whyte, F. Muntoni, H. Lee, S. F. Nelson, L. Yu and K. P. Campbell, *Science*, 2013, **341**, 896.
10 I. Gerin, *et al.*, *Nat. Commun.*, 2016, **7**, 11534.
11 M. Kanagawa, *et al.*, *Cell Rep.*, 2016, **14**, 2209.
12 J. L. Praissman, *et al.*, *eLife*, 2016, **5**, e14473.
13 M. O. Sheikh, *et al.*, *Nat. Commun.*, 2022, **13**, 3617.
14 J. M. Ervasti and K. P. Campbell, *J. Cell Biol.*, 1993, **122**, 809.
15 Y. Hara, M. Kanagawa, S. Kunz, T. Yoshida-Moriguchi, J. S. Satz, Y. M. Kobayashi, Z. Zhu, S. J. Burden, M. B. Oldstone and K. P. Campbell, *Proc. Natl. Acad. Sci. U. S. A.*, 2011, **108**, 17426.
16 T. Yang, *et al.*, *bioRxiv*, 2023, preprint, DOI: **10.1101/2023.12.20.57236**.
17 M. Kufleitner, L. M. Haiber and V. Wittmann, *Chem. Soc. Rev.*, 2023, **52**, 510.
18 M. Riemersma, *et al.*, *Chem. Biol.*, 2015, **22**, 1643.
19 C. Singh, E. Glaab and C. L. Linster, *J. Biol. Chem.*, 2017, **292**, 1005.
20 S. Hoshino, H. Manya, R. Imae, K. Kobayashi, M. Kanagawa and T. Endo, *J. Biochem.*, 2024, **175**, 418.
21 S. H. Yu, M. Boyce, A. M. Wands, M. R. Bond, C. R. Bertozzi and J. J. Kohler, *Proc. Natl. Acad. Sci. U. S. A.*, 2012, **109**, 4834.
22 H. Y. Tan, R. Eskandari, D. Shen, Y. Zhu, T.-W. Liu, L. I. Willems, M. G. Alteen, Z. Madden and D. J. Vocadlo, *J. Am. Chem. Soc.*, 2018, **140**, 15300.
23 B. Schumann, *et al.*, *Mol. Cell*, 2020, **78**, 824.
24 C. Périgaud, G. Gosselin, I. Lefebvre, J.-L. Girardet, S. Benzaria, I. Barber and J.-L. Imbach, *Bioorg. Med. Chem. Lett.*, 1993, **3**, 2521.
25 U. Pradere, E. C. Garnier-Amblard, S. J. Coats, F. Amblard and R. F. Schinazi, *Chem. Rev.*, 2014, **114**, 9154.
26 Z. Xie, L. Lu, Z. Wang, Q. Luo, Y. Yang, T. Fang, Z. Chen, D. Ma, J. Quan and Z. Xi, *Eur. J. Med. Chem.*, 2022, **243**, 114796.
27 J. F. A. Pijnenborg, E. A. Visser, M. Noga, E. Rossing, R. Veizaj, D. J. Lefeber, C. Büll and T. J. Boltje, *Chemistry*, 2021, **27**, 4022.
28 J. F. A. Pijnenborg, E. Rossing, J. Merx, M. J. Noga, W. H. C. Titulaer, N. Eerden, R. Veizaj, P. B. White, D. J. Lefeber and T. J. Boltje, *Nat. Commun.*, 2021, **12**, 7024.
29 Y. Norimura, D. Yamamoto and K. Makino, *Org. Biomol. Chem.*, 2017, **15**, 640.
30 J. A. Delbrouck, A. Tikad and S. P. Vincent, *Chem. Commun.*, 2018, **54**, 9845.
31 G. Yang, X. Ding and F. Kong, *Tetrahedron Lett.*, 1997, **38**, 6725.
32 L. D. Murphy, K. E. Huxley, A. Wilding, C. Robinson, Q. P. O. Foucart and L. I. Willems, *Chem. Sci.*, 2023, **14**, 5062.
33 Z. Li, I. P. Michael, D. Zhou, A. Nagy and J. M. Rini, *Proc. Natl. Acad. Sci. U. S. A.*, 2013, **110**, 5004.
34 J. H. Yoon, R. Xu and P. Martin, *PLoS Curr.*, 2013, **5**, DOI: **10.1371/currents.md.3756b4a389974dff21c0cf13508d3f7b**.
35 R. Harrison, P. G. Hitchen, M. Panico, H. R. Morris, D. Mekhaiel, R. J. Pleass, A. Dell, J. E. Hewitt and S. M. Haslam, *Glycobiology*, 2012, **22**, 662.
36 H. Yagi, C. W. Kuo, T. Obayashi, S. Ninagawa, K. H. Khoo and K. Kato, *Mol. Cell. Proteomics*, 2016, **15**, 3424.
37 R. M. J. Thewissen, *et al.*, *JIMD Rep.*, 2024, **65**, 171.
38 M. P. Cataldi, P. Lu, A. Blaeser and Q. L. Lu, *Nat. Commun.*, 2018, **9**, 3448.